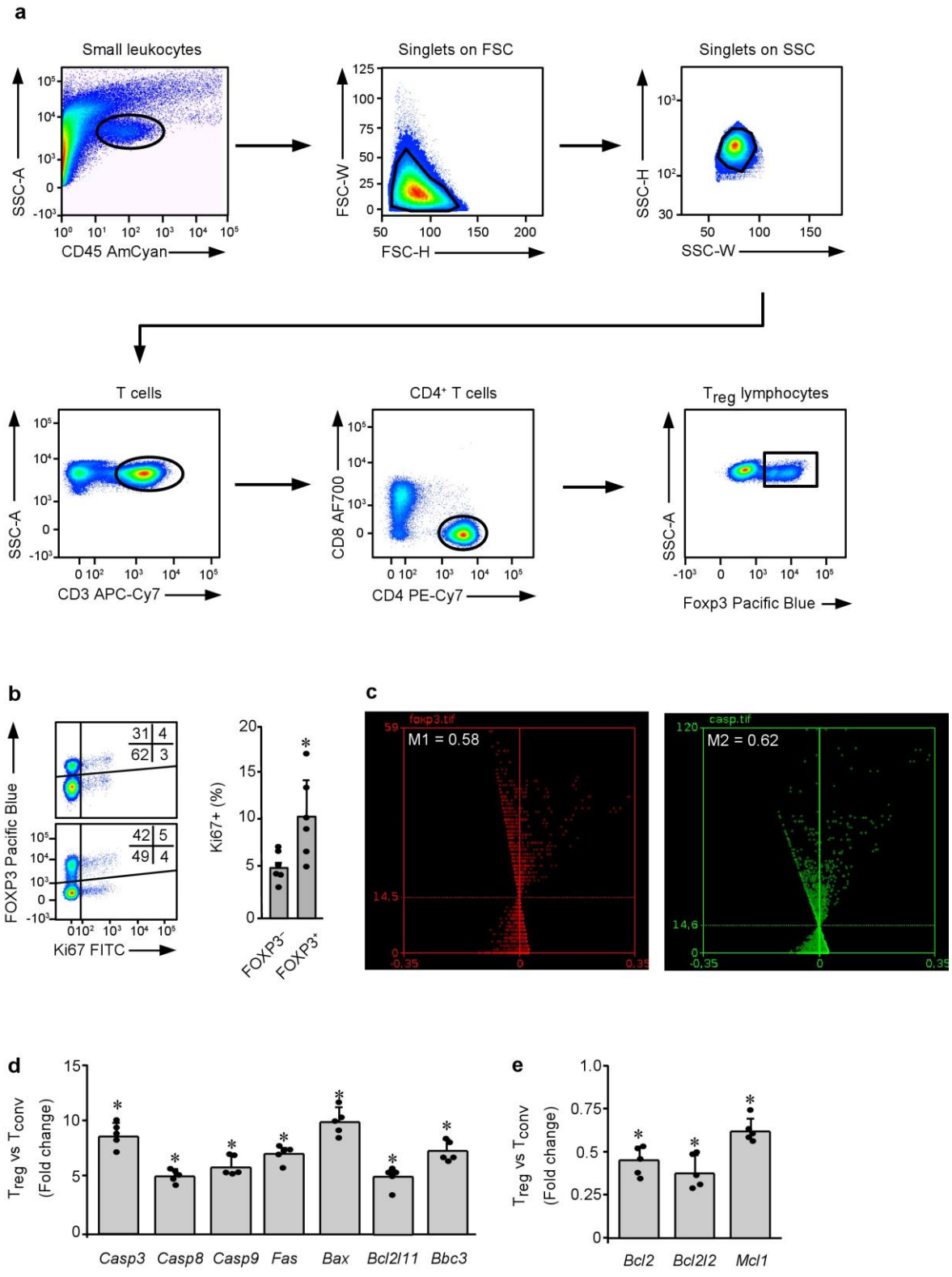

Supplementary Figure 1

Expression of apoptosis-related genes in tumor T_{reg} cells.
(**a**) Identification of FOXP3 T_{reg} cells by FACS. $CD45^+$ cells were gated as enriched lymphoid cell populations with low-granularity. Singlet cells were gated on the basis of forward and side scatter W and H parameters. Next, T cell subsets were identified on the basis

of CD3, CD4, and CD8 staining. T_{reg} cells were identified as $FOXP3^+CD4^+$ T cells. $FOXP3^-CD4^+$ T cells were conventional T cells. (**b**) Ki67 expression in tumor infiltrating T cell subsets. Ki67 expression was detected in human ovarian cancer infiltrating $FOXP3^+$ and $FOXP3^-CD45^+CD3^+CD4^+$ cells. Ki67 expression was shown in $CD4^+$ T cells from two representative ovarian cancer specimens (left panel) and in $FOXP3^-$ and $FOXP33^+CD4^+$ T cell subsets (right panel). mean ± s.d., n = 10, Student's t-test, * $P < 0.05$. (**c**) Split Manders' coefficient plot depicts the colocalization of FOXP3 (red) and cleaved CASP3 (green) in human ovarian cancer section. One representative of 10 is shown. (**d,e**) Effect of mouse tumor medium on T_{reg} cell gene expression. Normal mouse GFP^+ T_{reg} cells and GFP^- conventional T cells were cultured with MC38-medium for 24 hours. Expression of pro-apoptotic (**d**) and anti-apoptotic (**e**) genes was quantified by real-time PCR. The level of each gene in T_{reg} cells was normalized to that in conventional T cells. Data are shown as mean ± s.d., n = 5; Student's t-test, *$P < 0.05$.

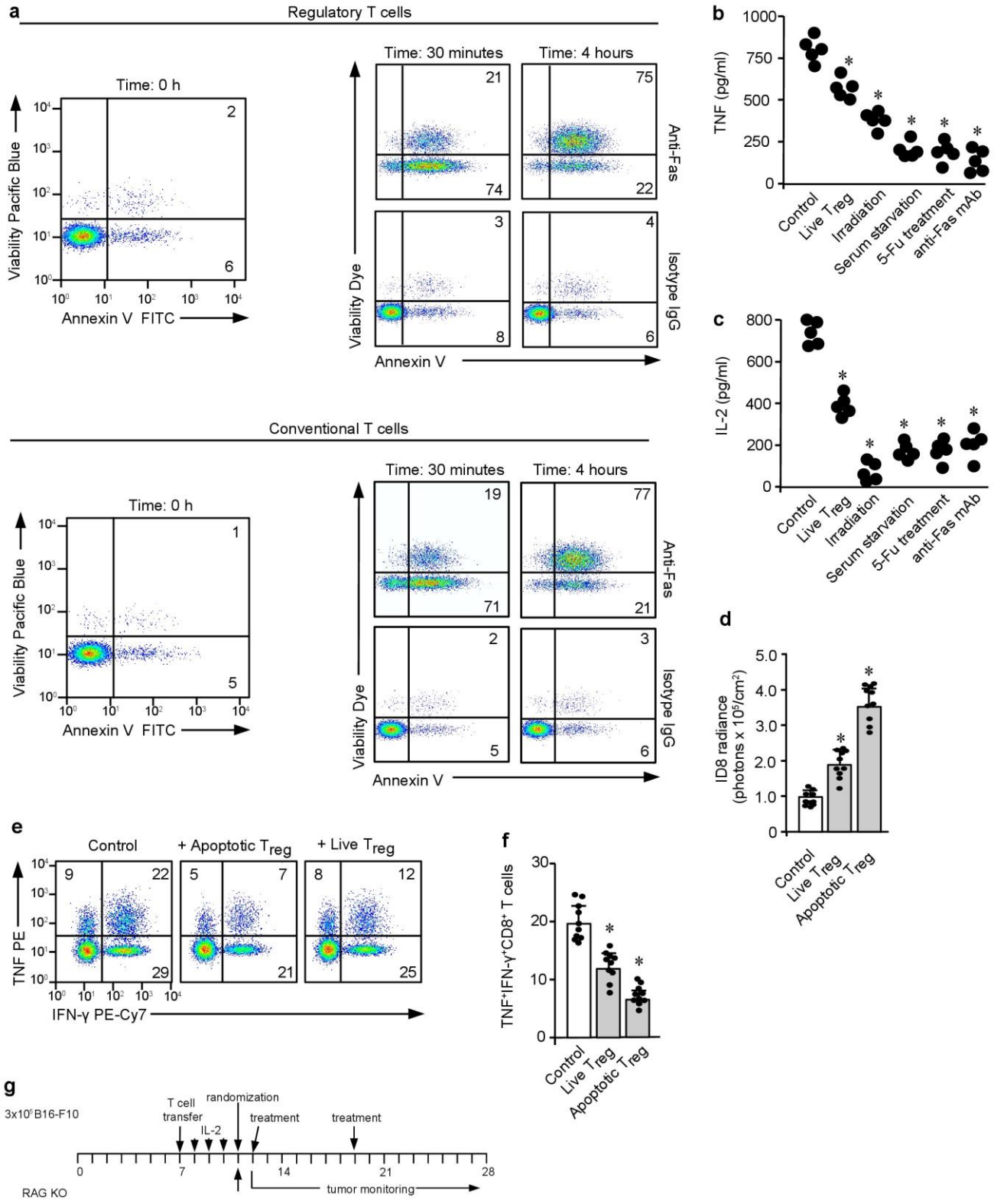

Supplementary Figure 2

Suppressive activity of mouse live and apoptotic T_{reg} cells.
(**a**) Representative dot plots show T_{reg} and T_{conv} apoptosis induced by anti-FAS mAb Jo-1. Annexin V expression was analyzed by FACS at 30 minutes and 4 hours. (**b,c**) Mouse T_{reg} apoptosis was induced by different conditions. T cell suppressive assay was

performed with these apoptotic T_{reg} cells. T cell TNF (**b**) and IL-2 (**c**) were measured on day 3 by ELISA, $n = 5$, Student's t-test, $^*P < 0.05$. (**d-f**) Effect of live and apoptotic T_{reg} cells on ID8-OVA tumor immunity. ID8-OVA-bearing mice were treated with live and apoptotic T_{reg} cells. Tumor growth is shown as final bioluminescent signal quantification (**d**). Effector T cell cytokine expression (**e, f**) was detected in cancer ascites fluid. Data presented as mean ± s.d., $n = 10$ animals per group; ANOVA with Dunett post-hoc test, $^*P < 0.05$. (**g**) Scheme of pmel-specific B16-F10 model. B16-F10 tumor bearing $RAG2^{-/-}$ mice received Pmel-specific T cells and intratumoral apoptotic Treg cell administration as indicated.

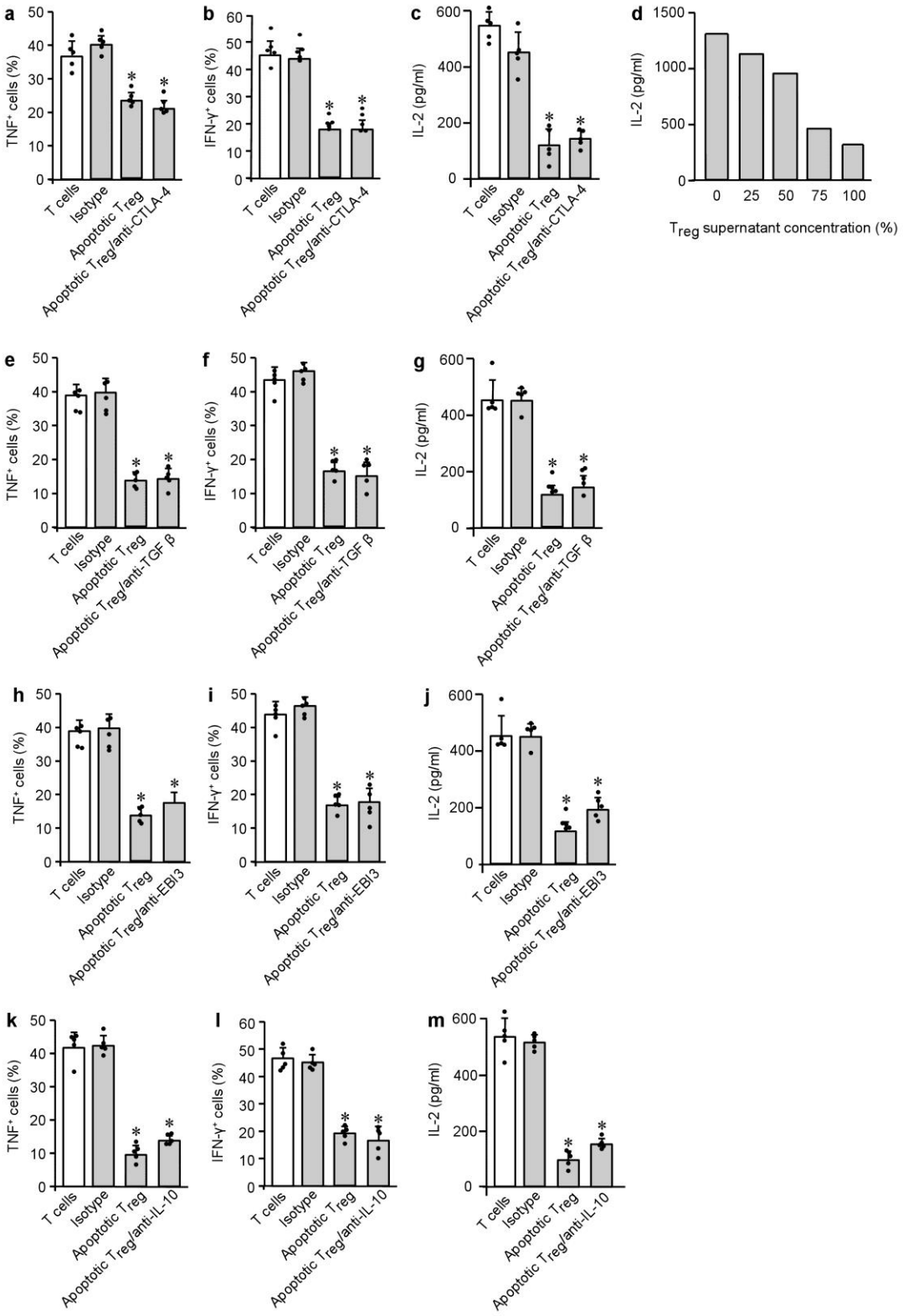

Supplementary Figure 3

Apoptotic T_{reg} cells mediated immunosuppression via small and non-protein molecules.
(**a-c**) Effect of CTLA-4 blockade on apoptotic Treg-mediated immunosuppression. T cell immunosuppressive assay was performed with apoptotic T_{reg} cells in the presence of anti-CTLA4 mAb. TNF (**a**) and IFN-γ (**b**) were analyzed by FACS on day 3 and IL-2 (**c**) was

detected by ELISA on day 5 $n = 5$, ANOVA with Dunett's post-hoc test, $^*P < 0.05$. (**d**) Effect of apoptotic Treg supernatants on T cell IL-2 production. Apoptotic Treg supernatants were collected at 6 hour time point and were added into T cell culture. T cell IL-2 was measured by ELISA. One of 3 experiments is shown. (**e-m**) Effect of the indicated cytokine blockade on apoptotic Treg cell-mediated immunosuppression. T cell immunosuppressive assay was performed with apoptotic T_{reg} cells in the presence of anti-TGF-β (**e-g**), anti-EBI3 (**h-j**), and anti-IL-10 (**k-l**) mAbs. TNF (**e, h, k**) and IFN-γ (**f, I, l**) were analyzed by FACS on day 3. IL-2 (**g, j, m**) was detected by ELISA on day 5. $n = 5$, ANOVA with Dunett's post-hoc test, $^*P < 0.05$.

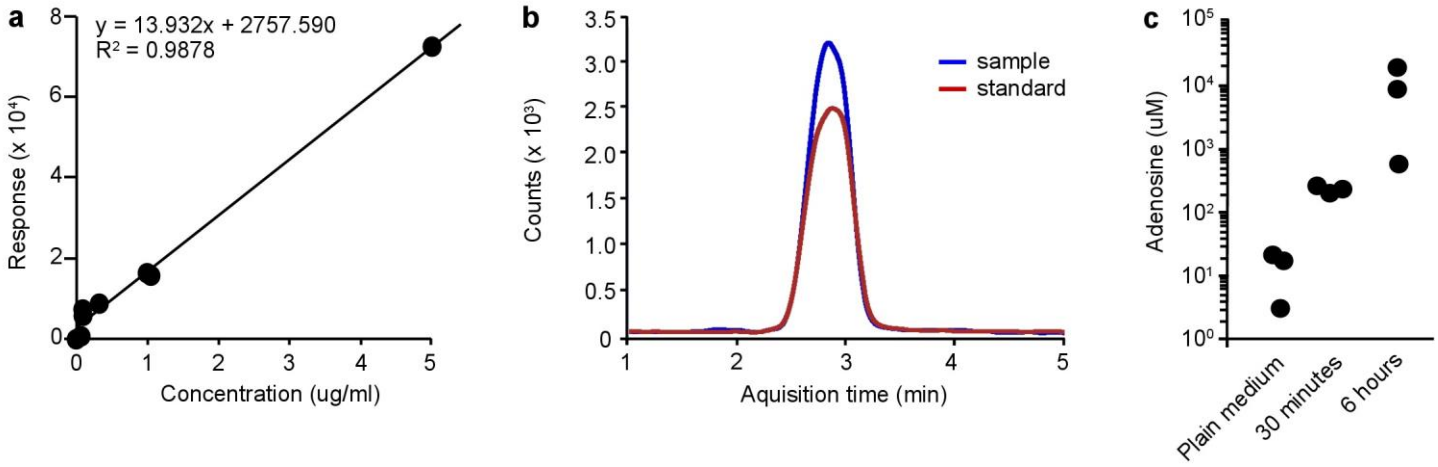

Supplementary Figure 4

Adenosine production by apoptotic T_{reg} cells.

T_{reg} cell apoptosis was induced with anti-Fas mAb. Adenosine was measured by mass spectrometry in supernatants collected at different time points. Based on the standard curve (**a**) and the extracted ion changed chromatogram (**b**), adenosine was detected at 0.5 and 6 hours after induction of apoptosis (**c**). One of 3 independent experiments is shown.

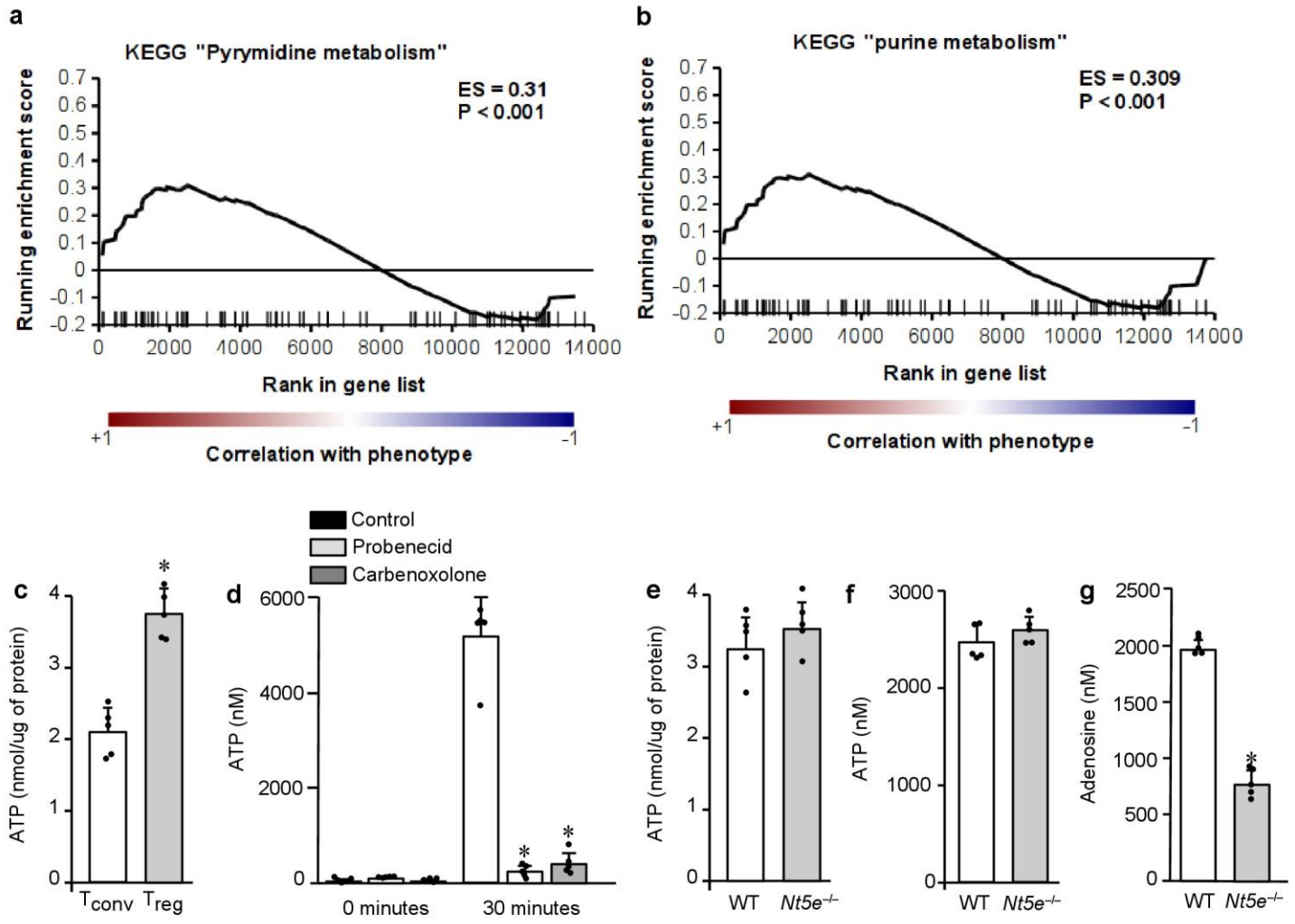

Supplementary Figure 5

The metabolic profile of T_{reg} cells.

(**a,b**) Purine (**a**) and pyrimidine (**b**) associated metabolism pathway in tumor associated T_{reg} cells. GSEA analysis was performed in tumor associated T_{reg} cells compared to conventional T cells at GSE55705 data set from GEO database. (**c**) Intracellular content of ATP in T_{reg} cells and T_{conv}. ATP level was measured in cell lysates with comparable amount of protein by colorimetric assay. Data shown as mean ± s.d., Student's t-test, $n = 5$, $^*P < 0.05$. (**d**) Effect of the pannexin-1 channel inhibitors on apoptotic T_{reg} ATP release. Apoptosis was induced by anti-FAS treatment in the presence or absence of inhibitors probenecid and carbenoxolone. ATP in the supernatants was measured by colorimetric assay. Data presented as mean ± s.d., Student's t-test, $n = 5$, $^*P < 0.05$ in comparison with control. (**e,f**) Intracellular (**e**) and released (**f**) ATP in live (**e**) and apoptotic (**f**) wild-type or *Nt5e*$^{-/-}$ mouse T_{reg} cells. ATP level in whole cells was normalized to total protein expression (**e**). ATP in apoptotic T_{reg} cell supernatants was shown at 30 minutes (**f**). $n = 5$, paired Student's t-test, $^*P > 0.05$. (**g**) Adenosine production by wild-type and *Nt5e*$^{-/-}$ apoptotic T_{reg} cells. T_{reg} cell apoptosis was induced with anti-FAS and the supernatants were collected at 30 minutes. After deproteinization, adenosine was measured by colorimetric assay. Data shown as mean ± s.d., $n = 5$, Student's *t*-test, $^*P < 0.05$.

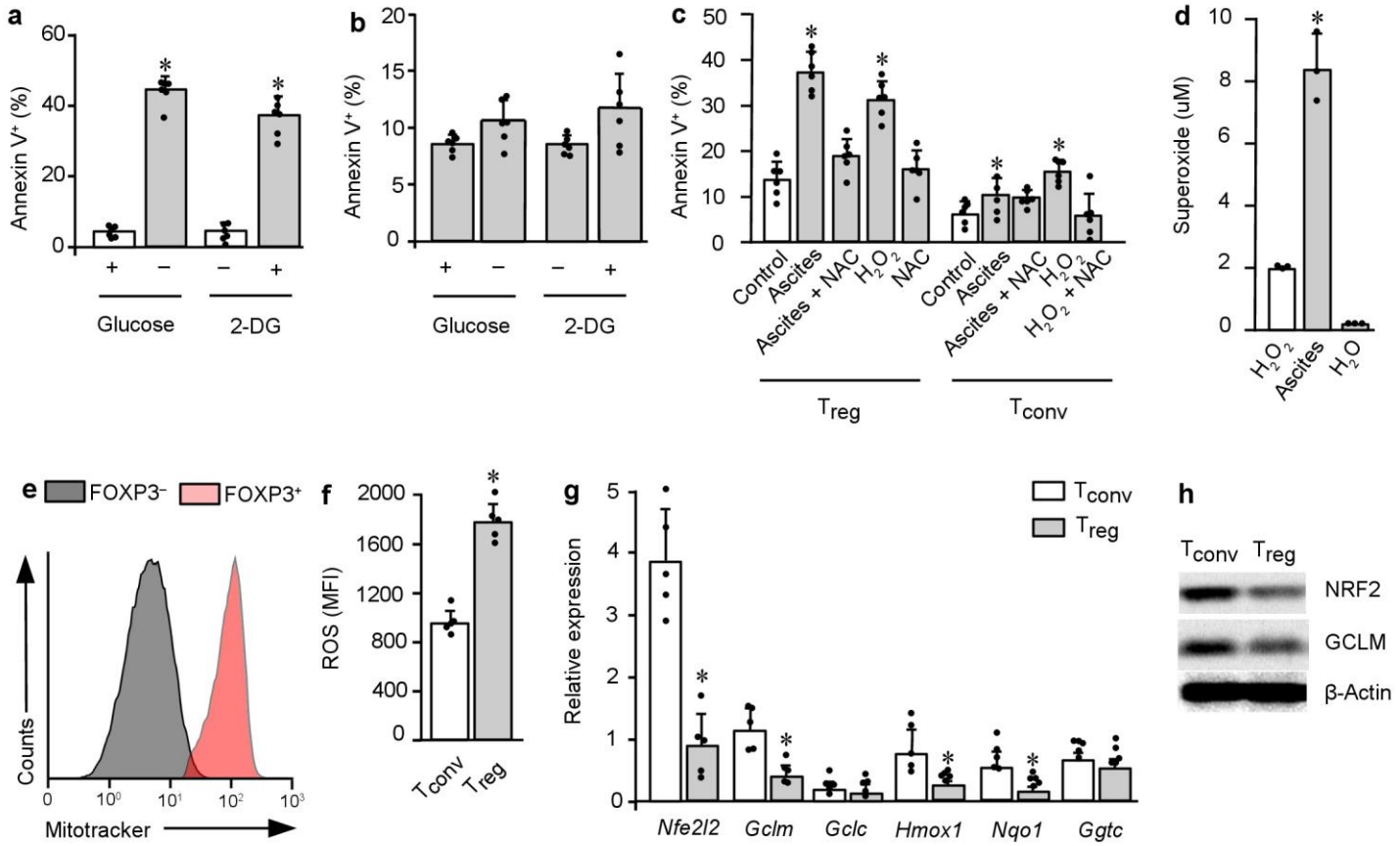

Supplementary Figure 6

The effect of tumor oxidative stress on T_{reg} cells.
(**a,b**) Effect of glucose restriction and 2-DG on conventional T cell (**a**) and Treg (**b**) apoptosis. Human T cell subsets were cultured with or without glucose or 2-DG for 24 hours. Annexin V^+ T cells were measured by flow cytometry. One-way ANOVA with Dunnet's post-hoc test, $*P < 0.05$. (**c**) Effect of human ovarian cancer ascites on Treg apoptosis. Mouse T_{reg} cells and conventional T cells (Tconv) were co-cultured with 50% ascites from intraperitoneal ID8 ovarian cancer bearing animals or hydrogen peroxide for 24 hours. Additional cultures were treated with NAC as a free radical scavenger. Annexin V^+ T_{reg} cells and Tconv were analyzed by flow cytometry. Data presented as mean ± s.d., $n = 6$, $*P < 0.05$. (**d**) Superoxide level in human ascites. The concentration of superoxide was measured with colorimetric test. Water contains 2 μM H_2O_2 as a positive control. Data are shown as mean ± s.d., $n = 3$. (**e**) Mitochondrial load of mouse T_{reg} cells. The cells were treated with fluorescent mitochondrial activity dye (Mitotracker) and analyzed by flow cytometry. One of 3 assays is shown. (**f**) Level of reactive oxygen species (ROS) in ovarian cancer infiltrating conventional T cells and T_{reg} cells. The level of ROS was tested by CellROX Green and ROS content was shown as mean fluorescence intensity. Data shown as mean ± s.d., $n = 5$, Student's *t*-test, $*P < 0.05$. (**g,h**) Expression of human Nrf2 and NRF2-associated genes and protiens in T_{reg} cells. *Nfe2l2* and NRF2-associated gene transcripts (**g**) and proteins (**h**) were determined in T cell subsets by real-time PCR and immunoblotting, respectively. Data presented as mean ± s.d., $n = 5$, paired Student's t-test, $*P < 0.05$

Supplementary Table 1. Enrichment of Gene Ontology Terms in T_{reg} cells compared to conventional T cells in B16 melanoma tissues (data series GSE55705).

Up-regulated genes			
GO term	GO ID	raw p-value	adj. p-value
electron transport chain	GO:0022900	2.24e-07	0.0008
apoptotic process	GO:0006915	2.47e-06	0.0031
generation of precursor metabolites and energy	GO:0006091	3.57e-06	0.0031
programmed cell death	GO:0012501	3.64e-06	0.0031
death	GO:0016265	4.38e-06	0.0031
cell death	GO:0008219	5.50e-06	0.0032
induction of apoptosis	GO:0006917	0.0001	0.0292
regulation of apoptotic process	GO:0042981	0.0001	0.0292
induction of programmed cell death	GO:0012502	7.68e-05	0.0292
organophosphate metabolic process	GO:0019637	0.0001	0.0292
Down-regulated genes			
RNA metabolic process	GO:0016070	1.04e-10	2.79e-07
cellular macromolecule metabolic process	GO:0044260	9.61e-10	8.59e-07
nucleic acid metabolic process	GO:0090304	9.35e-10	8.59e-07
nucleobase-containing metabolic process	GO:0006139	1.40e-09	9.39e-07
gene expression	GO:0010467	5.97e-09	2.29e-06
cellular metabolic compound metabolic process	GO:0006725	5.42e-09	2.29e-06
heterocycle metabolic process	GO:0046483	5.76e-09	2.29e-06
RNA processing	GO:0006396	1.69e-08	5.67e-06
cellular nitrogen compound metabolic process	GO:0034641	2.74e-08	8.17e-06
organic cyclic compound metabolic process	GO:1901360	4.32e-08	1.16e-05

Note: Enrichment of Gene Ontology Terms for biological processes was analyzed for significantly up- and down-regulated genes on a background of Affymetrix Mouse 420a v. 2.0 platform (GPL8321). The table contains top 10 significantly enriched biological processes terms.

Supplementary Table 2. Enrichment of KEGG Pathways in T_{reg} cells compared to conventional T cells in B16 melanoma tissues (data series GSE55705).

Up-regulated pathways		
Pathway name	raw p-value	adj. p-value
metabolic pathways	1.07e-62	1.99e-60
Huntington's disease	1.53e-25	1.42e-23
Alzheimer's disease	3.28e-24	2.03e-22
Parkinson's disease	2.31e-21	1.07e-19
oxidative phosphorylation	2.58e-19	9.60e-18
pathways in cancer	5.97e-16	1.85e-14
MAPK signaling pathway	8.74e-14	2.09e-12
cell cycle	8.97e-14	2.09e-12
proteasome	5.58e-13	1.15e-11
p53 signaling pathway	3.86e-10	4.22e-09
pyrimidine metabolism	6.14e-10	6.34e-09
purine metabolism	5.71e-06	2.21e-05
apoptosis	2.11e-05	7.11e-05
chemokine signaling pathway	4.59e-12	8.54e-11
pyruvate metabolism	0.0004	0.0011
fatty acid metabolism	0.0006	0.0013
Down-regulated pathways		
ribosome	3.18e-09	5.15e-07
ribosome biogenesis in eukarytes	0.0005	0.0324
RNA transport	0.0006	0.0324
spliceosome	0.0060	0.2430
acute myleoid leukemia	0.0241	0.7128
valine, leucine and isoleucine biosynthesis	0.0286	0.7128
aldosterone-regulated sodium reabsorption	0.0308	0.7128
RNA degradation	0.0363	0.7351
colorectal cancer	0.0442	0.7956
apoptosis	0.3392	0.7990

Note: Enrichment of KEGG Pathways were analyzed for significantly up- and down-regulated genes on a background of mouse genome. The table contains top 10

enriched pathways and some other statistically enriched pathways. Additionally, of the up-regulated pathways there are some significantly enriched pathways (below dashed line), but not in top 10.

Supplementary Table 3. Primers for real-time PCR analysis (5' → 3')

Gene ID (GeneBank)	Human Forward	Reverse
Bbc3	TGGGTGAGACCCAGTAAGGA	CTCCCTGGGGCCACAAATCT
BclxL	AGACCCCCAGTGCCATCAAT	CATCCAAACTGCTGCTGTGCG
Bcl2	GGAGGCTGGGATGCCTTTGT	AAAGCCAGCTTCCCCAATGA
Bim	GGTCTGCAGTTTGTTGGAGC	ATGGAAGCCATTGCACTGAGA
Bax	TTTGCTTCAGGGTTTCATCCA	CTGGAGACAGGGACATCAGT
Casp3	GCTCTGGTTTTCGGTGGGTG	ACCACGGCAGGCCTGAATAAT
Casp8	AGCCCTGCTGAATTTGCTAGTC	CAGGAGAATATAATCCGCTCCAC
Casp9	CAGGCCCCATATGATCGAGG	TCAAGAGCACCGACATCACC
Fas	CCCTGTCCTCCAGGTGAAAG	AGACAAAGCCACCCCAAGTT
Gapdh	CTCCTCCTGTTCGACAGTCA	TGCAGGAGGCATTGCTGATG
Gclc	ACCAGACCGGCAAAGAGAAG	CCAGGACAGCCTAATCTGGG
Gclm	AAGCACTTTCTCGGCTACGA	TCATGAAGCTCCTCGCTGTG
Ggct	CAGAGAGGATCCACCTCCGA	TAACCCCTTCTTGCTCATCCAG
Hmox1	GTGCCACCAAGTTCAAGCAG	CACGCATGGCTCAAAAACCA
Mcl1	GACTTTTGGCTACGGAGAAGGA	AACTCCACAAACCCATCCCAG
Nqo1	GCTGGTTTGAGCGAGTGTTC	CTGCCTTCTTACTCCGGAAGG
Nrf2	CGACCTTCGCAAACAACTCT	TGTGGGCAACCTGGGAGTAG
Gene ID (GeneBank)	Mouse Forward	Reverse
Bbc3	CATAGAGCCACATGCGAGCG	TGCTCTTCTTGTCTCCGCCG
BclxL	ACCTCCTCCCCGACCTATGA	CTATCTCCGGCGACCAGCAA
Bcl2	CAGCCTGAGAGCAACCCAAT	TATAGTTCCACAAAGGCATCCCAG
Bim	CTGCGAGCTGTGTTCCACTT	ATGGAAGCCATTGCACTGAGA
Bax	GAGCTGCAGAGGATGATTGC	CTTGGATCCAGACAAGCAGC
Casp3	GAGCTTGGAACGGTACGCTA	GCGAGATGACATTCCAGTGC

Casp8	AGAAAGCGAAGCAGCCTATGG	TAGAAGAGCTGTAACCTGTGGC
Casp9	GCGCGACATGATCGAGGATA	TGGTCTTTCTGCTCACCACC
Fas	TGCTTGCTGGCTCACAGTTA	GTTCCATGTTCACACGAGGC
Gapdh	CCCTTAAGAGGGATGCTGCC	TACGGCCAAATCCGTTCACA
Gclc	TTGGGTCGCAAGTAGGAAGC	GTTAGAGTACCGAAGCGGGG
Gclm	TGGGCACAGGTAAAACCCAA	CACCCTGATGCCTAAGCCAA
Ggct	CGCCTGCAGGACTTTAAGC	AAGCCGATCGGATACAAGCA
Hmox1	GAGCAGAACCAGCCTGAACT	AAATCCTGGGGCATGCTGTC
Mcl1	CAAAGAGGCTGGGATGGGTTT	CCCTATTGCACTCACAAGGC
Nqo1	CCGATTCAGAGTGGCATCCT	GAGCAATTCCCTTCTGCCCT
Nrf2	TTGCCCTAGCCTTTTCTCCG	ATGTGGGCAACCTGGGAGTA